

In silico screening of JAK-STAT modulators from the antiviral plants of Indian traditional system of medicine with the potential to inhibit 2019 novel coronavirus

Pukar Khanal (✉ pukarkhanal58@gmail.com)

Department of Pharmacology and Toxicology, KLE College of Pharmacy Belagavi, KLE Academy of Higher Education and Research, Belagavi-590010, Karnataka, India <https://orcid.org/0000-0002-8187-2120>

Taaza Duyu

Department of Pharmacology and Toxicology, KLE College of Pharmacy Belagavi, KLE Academy of Higher Education and Research, Belagavi-590010, Karnataka, India

BM Patil (✉ bmpatil59@hotmail.com)

Department of Pharmacology and Toxicology KLE College of Pharmacy, Belagavi, KLE Academy of Higher Education and Research (KAHER), Belagavi-590010, India

Yadu Nandan Dey (✉ yadunandan132@gmail.com)

Adamas University, School of Pharmaceutical Technology, Kolkata, India

Ismail Pasha

Department of Pharmacology, Orotta College of Medicine and Health Sciences, Asmara University, Asmara, Eritrea

Rohini S. Kavalapure

Department of Pharmaceutical Chemistry, KLE College of Pharmacy, Belagavi, KLE Academy of Higher Education and Research (KAHER), Belagavi-590 010, India

Research Article

Keywords: 3CLpro, anti-viral, COVID-19, JAK-STAT pathway, PLpro

Posted Date: May 28th, 2020

DOI: <https://doi.org/10.21203/rs.3.rs-32233/v1>

License:  This work is licensed under a Creative Commons Attribution 4.0 International License.

[Read Full License](#)

Version of Record: A version of this preprint was published at 3 Biotech on February 8th, 2021. See the published version at <https://doi.org/10.1007/s13205-021-02664-4>.

Abstract

Aim. The present study was aimed to identify the lead hits from reported anti-viral Indian medicinal plants to modulate the proteins through the JAK-STAT pathway and to identify the proteins that share the domain with coronavirus (COVID19) associated proteins i.e. 3CLpro, PLpro, and spike protein. *Methods.* The reported anti-viral plants were screened from the available databases and published literature; their phytoconstituents were retrieved, gene-expression was predicted and the modulated proteins in JAK-STAT pathway were predicted. The interaction between proteins was evaluated using STRING and the network between phytoconstituents and proteins was constructed using Cytoscape. The druglikeness score was predicted using MolSoft and the ADMET profile of phytoconstituents was evaluated using admetSAR2.0. The domain of three proteins i.e. 3CLpro, PLpro, and spike protein of coronavirus was compared using NCBI blastP against the RCSB database. *Results.* The majority of the phytoconstituents from the anti-viral plants were predicted to target TRAF5 protein in the JAK-STAT pathway; among them, vitexilactone was predicted to possess the highest druglikeness score. Proteins targeted in the JAK-STAT pathways were also predicted to modulate the immune system. Similarly, the docking study identified sesaminol 2-O- β -D-gentiobioside to possess the highest binding affinity with spike protein. Similarly, phylogeny comparison also identified the common protein domains with other strains of microbes like murine hepatitis virus strain A59, avian infectious bronchitis virus, and porcine epidemic diarrhea virus CV777. *Conclusion.* Although, the present study is based on computer simulations and database mining, it provides two important aspects in identifying the lead hits against coronavirus. First, targeting the JAK-STAT pathway in the corona-infected host by folk anti-viral agents can regulate the immune system which would inhibit spreading the virus inside the subject. Secondly, the well-known targets of coronavirus i.e. 3CLpro, PLpro, and spike protein share some common domains with other proteins of different microbial strains.

1. Introduction

Recently, CoV Disease-19 (COVID-19) has emerged as a powerful public enemy throughout the world leading to the death of a huge number of the population. Originating from China, COVID-19 drastically spread throughout the world in a quick period and affected more than 50 different countries [1]. World Health Organization (WHO) has declared COVID-19 as “Pandemic” and has suggested preventive approaches like social isolation and intensive care of patients [2]. Earlier reports indicate the deregulation of the JAK-STAT pathway when coronavirus invades the host by affecting the synthesis of type I IFNs via the activation of IRF3/7 which promotes IFN-stimulated genes. Likewise, the stimulation of IFN by host cells helps in immune modulation and also prevents the spreading of viruses [3]. Hence, modulating the expression of the multiple proteins of the JAK-STAT pathway would regulate the production of IFN-associated genes and could help in the minimization of virus spreading. Further, coronavirus is composed of multiple proteins that play an important role in entering and replicating inside the host. Among them, 3C-like protease (3CLpro), papain-like protease (PLpro), and spike protein are the choice of proteins that were majorly studied. 3CLpro alters the ubiquitin system and also modifies the functional

protein by incorporating the viral polypeptides [4]. PLpro has a role to process pp1a and pp1ab into the replicase proteins; plays an important task in the viral life cycle [5]. Likewise, spike protein utilizes angiotensin-converting enzyme 2 as a receptor to enter inside the cell [6]. Hence, these three proteins of coronavirus could be the targets of interest for investigations.

Further, this pandemic disease COVID-19 is still spreading rapidly. Hence, it is urgent to identify the therapeutic agents that either have a preventive or curative role against the disease. Though multiple investigations are initiated worldwide to identify the specific agents against the COVID-19, it may take more time to completely eradicate this. Although no specific therapy has been identified to coronavirus till date, the approach for managing COVID-19 can be made via two approaches i.e. (a) trying to re-regulate the altered JAK-STAT pathway towards homeostatic condition by using multiple compounds and (b) secondly, utilization of well-reported molecules against 3CLpro, PLpro, and spike protein by utilizing the compounds that act on their homologous proteins.

Indian traditional system of medicines described many antiviral plants that are effective in controlling viral infection. In view of the scarcity of treatment to combat COVID-19, it was thought to identify the potential lead hit molecules from Indian medicinal plants (anti-viral agents) to act over the JAK-STAT pathway and identify the homologous proteins of 3CLpro, PLpro, and spike protein using open source databases.

2. Materials And Methods

2.1. Compounds mining and their gene expression study

The Indian traditional medicines as anti-viral agents were identified by using the open-source database and published literature. The list of each phytoconstituent was retrieved using the ChEBI database (<https://www.ebi.ac.uk/chebi>) and their SMILES were queried in DIGEP-Pred [7] to identify the probable expression of genes based on mRNA prediction at the probable activity (Pa)>0.5. A complete datasheet was constructed composing the list of plants, their phytoconstituents, and their expression profile.

2.2. Identification of proteins involved in the JAK-STAT pathway

The proteins modulated by phytoconstituents involved in the JAK-STAT pathway were identified relating to the JAK-STAT signaling pathway from the KEGG pathway database (<https://www.genome.jp/kegg/pathway.html>); pathway ID: hsa04630. The "Pivot Table" from excel was used to identify the phytoconstituents targeting the highest number of proteins in the JAK-STAT pathway and protein targeted by the large number of phytoconstituents. Multiple keywords "STAM, JAK, TC-PTP, SHP1, STAT, SHP2\GRB, PI3K, AKT, SOS, IRF9, Ras, Raf, mTOR, PIAS, SLIM, CBP/300, CIS, Bcl-2, Bcl-XL, c-Myc, p21, AOX, GFAP, SOCS, MCL1, PIM1, and CycD" were used to identify the modulators of the JAK-STAT pathway with reference to KEGG pathway; hsa04630.

2.3. Enrichment analysis, network construction, and hit identification

Enrichment analysis of the expressed proteins in the JAK-STAT pathway was performed by querying a list of modulated proteins using STRING [8]. Further, probable biological processes, cellular component and KEGG pathways were identified. The network interaction of phytoconstituents and modulated proteins (JAK-STAT pathway) was constructed using Cytoscape 3.7.1 [9]. The constructed network was analyzed based on edge count by treating network as directed and setting the node size as “low values to small sizes” and color as “low values to bright colors”. Then the protein targeted by the highest number of phytoconstituents was further chosen as a macromolecule for docking study.

2.4. Druglikeness and ADMET profiling of lead hits

Since Indian herbal treatments are taken orally; we attempted to predict the druglikeness score of hit phytoconstituents using MolSoft (<https://molsoft.com/mprop/>) which was based on Lipinski's Rule of Five by calculating molecular weight, number of hydrogen bond donor, number of hydrogen bond acceptor and logP value. Similarly, absorption, distribution, metabolism, excretion, and toxicity (ADMET) profile of lead hits were also calculated using admetSAR2.0 [10].

2.5. In silico molecular docking

The crystallographic protein of TRAF5 for human was not found in RCSB (<https://www.rcsb.org/>) protein databank. Hence, homology modeling was performed for TRAF5 using the FASTA sequence of AAH29600.1 as a query sequence against TRAF5 from *Mus musculus* as a template (PDB: 4GJH) using SWISS-MODEL [11]. Pre-complexed hetero-atoms from the retrieved target were removed using Discovery studio 2019 [12] and saved in .pdb format. The corresponding 3D structure of ligand molecules against TRAF5 was retrieved from the PubChem database (<https://pubchem.ncbi.nlm.nih.gov/>) in .sdf format, converted into .pdb format using Discovery studio 2019; drawn in Marvin sketch (<https://chemaxon.com/products/marvin>) and converted into 3D .pdb format if not available in PubChem database. The energy of each molecule was minimized using mmff94 forcefield [13] and converted into .pdbqt format. Autodock4 [14] was used to dock the identified ligand molecules with TRAF5. After docking, ten different poses were obtained; pose scoring minimum binding energy was chosen to visualize the ligand-protein interaction using Discovery studio. Further, we assessed the binding affinity of lead hits with 3clpro (PDB: 6LU7), PLpro (PDB: 4M0W) and spike proteins (homology modeled target, accession number: AVP78042.1 as query sequence and PDB: 6VSB as a template using SWISS-MODEL) as previously explained.

2.6. Phylogeny comparison of COVID-19 3clpro, PLpro and spike protein

The FASTA sequence of 3clpro (accession:1P9U_A, GI: 31616013), PLpro (accession: 4WUR_A, GI: 726969143) and spike protein (accession: AVP78042.1 GI: 1369125431) were retrieved from NCBI-protein and compared with RCSB protein bank database to identify the possible homologous proteins using BlastP [15].

3. Results

3.1. Identification of hits targeting the JAK-STAT pathway from a natural source

We screened 25 different herbal medicines; among them, 17 were chosen for further study i.e. *Abutilon indicum*, *Crescentia alata*, *Caesalpinia bonduc*, *Datura metel*, *Durio zibethinus*, *Evolvulus alsinoides*, *Garcinia mangostana*, *Indigofera tinctoria*, *Jatropha curcus*, *Leucas aspera*, *Orobancha corymbosa*, *Ricinus communis*, *Trichodesma indicum*, *Vitex trifolia*, *Wedelia Chinensis*, *Woodfordia fruticosa*, and *Wrightia tinctoria*; that were reported to possess anti-viral activity from which total 174 multiple phytoconstituents were retrieved from ChEBI database. Among them, 96 phytoconstituents were identified to modulate the proteins involved in the JAK-STAT pathway. Likewise, a total of 174 phytoconstituents were identified to regulate 807 genes; among them, 15 were from the JAK-STAT signaling pathway. Similarly, network analysis identified β -maaliene as a hit molecule to possess high gene expression from the JAK-STAT pathway and TRAF5 was identified to be majorly targeted (Figure 1). Similarly, GO gene analysis of proteins modulated in the JAK-STAT pathway is represented in Figure 2 reflects the highest number of gene regulation in biological process and were from the cytoplasm.

3.2. Enrichment analysis of JAK-STAT modulated proteins

Enrichment analysis of proteins relating to KEGG pathway database identified few pathways i.e. JAK-STAT signaling pathway, viral carcinogenesis, chronic myeloid leukemia, ErbB signaling pathway, apoptosis, Hepatitis B, Necroptosis, HTLV-I infection, NF-kappa B signaling pathway, Th17 cell differentiation, autophagy - animal, mTOR signaling pathway, chemokine signaling pathway, and Ras signaling pathway which; get regulated in viral infections (Table 1).

3.3. Druglikeness and ADMET profile of lead hits

Among 39 different phytoconstituents targeting TRAF5, vitexilactone was predicted to possess the highest druglikeness score i.e. 0.88. Among them, 18 compounds were predicted to possess a non-druglikeness character based on the rule of five. The druglikeness score of each phytoconstituent targeting TRAF5 is summarized in Table 2. Similarly, the ADMET profile of each phytoconstituent is represented in figure 3 as a heat map.

3.4. In silico molecular docking

Among 39 different phytoconstituents that interacted with TRAF5, sesaminol 2-O- β -D-gentiobioside was predicted to have the highest binding affinity i.e. -8.6 kcal/mol binding energy and five hydrogen bond interactions with GLN431, PHE429, TRP408 amino acids. However, vicenin-3 was predicted to have the highest number of hydrogen bond interactions i.e. nine with LYS500, ASP502, SER505, SER506, SER507, GLY520, SER519 amino acids; though scored comparatively lower binding affinity than sesaminol 2-O- β -D-gentiobioside i.e. binding energy: -6.6 kcal/mol (Table 3). The interaction of sesaminol 2-O- β -D-gentiobioside and vicenin-3 are represented in Figure 4.

Likewise, sesaminol 2-O- β -D-glucoside was predicted to have the highest binding affinity with 3clpro i.e. -9.2 kcal/mol with two hydrogen bond interactions with GLU166, THR190. Similarly, vicenin-3 was

predicted to have a binding affinity with 3clpro (binding energy: -8.2 kcal/mol) by forming five hydrogen interactions with GLY143, SER144, GLU166 (Table 4). The interaction of sesaminol 2-O-β-D-glucoside and vicenin-3 is represented in Figure 5.

Similarly, sesaminol 2-O-β-D-gentiobioside was predicted to possess binding energy of -8.5 kcal/mol with PLpro by four hydrogen bond interactions with THR75 and ASP77. However, taxine B was predicted to have the highest hydrogen bond interactions i.e. six with THR171, ARG167, GLU204, MET207, GLN233 though it scored comparatively lower binding energy i.e. -6.9 kcal/mol with PLpro (Table 5); interaction is represented in Figure 6.

Likewise, sesaminol 2-O-β-D-gentiobioside was predicted to have the highest binding affinity i.e. -9.7 kcal/mol binding energy with spike protein with the highest number of hydrogen bond interaction i.e. eight by interacting with THR47, LEU48, GLN825, ALA801, ALA803, PHE805, LYS807, and ASP811 (Table 6); interaction is represented in Figure 7.

3.5. Phylogeny comparison of COVID-19 3clpro, PLpro and spike protein

The blast result identified three different proteins (3C-like proteinase of porcine transmissible gastroenteritis coronavirus strain Purdue, replicase of transmissible gastroenteritis virus and Mpro Transmissible gastroenteritis virus) which are very similar to 3clpro based on maximum score, query cover, E-value and percentage identity. The alignments were also matched with some other proteins like Pedv 3c-like protease of diarrhea virus, replicative polyprotein 1ab of murine hepatitis virus strain A59 and purine nucleoside phosphorylase of *Toxoplasma gondii*. However, maximum matching was found with multiple strains of the coronavirus from different organisms. Similarly, the sequence of PLpro was found to be similar to previously reported papain-like protease from coronavirus in England and Jordan. We identified the matching of PLpro sequence with papain-like protease (Murine hepatitis virus strain A59) by 29.45%, replicase polyprotein 1ab (Murine hepatitis virus strain A59) by 29.13%, replicase polyprotein 1ab (Avian infectious bronchitis virus; strain Beaudette) by 27.11%, and nonstructural protein 3 (Avian infectious bronchitis virus; strain Beaudette) by 26.76%. Likewise, spike proteins from other viruses like Murine hepatitis virus strain A59, feline infectious peritonitis virus, infectious bronchitis virus, and porcine epidemic diarrhea virus CV777 were found to be similar with spike protein of coronavirus. Similarly, 47.06% of spike protein was found to be matched with Hepcidin; however, the E-value for this match was 5. Similarly, the dendrogram (Figure 8) represents the hierarchical clustering relationship of 3clpro, PLpro and spike protein with respective proteins.

4. Discussion

The present study dealt to identify the potential lead hits from anti-viral Indian traditional medicinal plants to regulate the JAK-STAT signaling pathway and identify the probable homologous proteins of COVID-19 3clpro, PLpro and spike protein concerning an available database.

Coronaviruses, a positive-sense RNA virus has a role in impairing pulmonary gas exchange which can primarily occur in the maladjusted immune system. Further, for the elimination of the coronavirus infection, the subject immune system plays an important role [3]. KEGG database also records the JAK-STAT pathway for multiple immunological disorders including JAK-STAT signaling for viruses (pathway entry: hsa04630). Hence, identification of lead hits to modulate the proteins of the JAK-STAT pathway from the medicinal plants can play an important role to maintain an immune system as a home remedy and may be helpful as a preventive approach to deal with corona infection. Further, we were interested to know if three targets of the coronavirus i.e. 3clpro, PLpro and spike protein can share their domain with any other pre-deposited protein molecules in the RCSB databank or not.

We queried the predeposited protein amino acid sequences of three proteins from COVID-19 i.e. 3clpro, PLpro, and spike protein and interestingly, we identified 3clpro protein to share its amino acid sequences with other microbial infections like PEDV main protease from Porcine epidemic diarrhea virus CV777. Further, PLpro was also found to share its protein alignment with replicase polyprotein 1ab of Murine hepatitis virus strain A59. Likewise, spike protein was also identified to have similar amino acid alignments with spike glycoprotein of Murine hepatitis virus strain A59. This observation suggests that analogs of protease inhibitors from procaine epidemic diarrhea could be the choice of the investigative molecule against 3clpro protein. Similarly, analogs of replicase polyprotein 1ab and spike glycoprotein of Murine hepatitis virus strain A59 could act over the PLpro and spike protein respectively towards coronavirus.

Enrichment analysis of modulated proteins from JAK-STAT pathways also identified multiple pathways to be regulated; could contribute to maintaining an immune system like apoptosis, necroptosis, Th1, and Th2 cell differentiation, NF-kappa B signaling pathway, Th17 cell differentiation, and chemokine signaling pathway. Coronavirus replication is linked with the membrane of the endoplasmic reticulum; increases the stress over it and leads to apoptosis via the process of unfolded protein response [16]. Likewise, the previous report suggests the corona virus-induced necrotic cell death due to multiple mechanisms like Rip3-induced oligomerization, MLKL dispensed cell death, necroptotic elements-induced human lung cell damage, lysosome-induced damage, and activation of multiple inflammasomes [17]. Hence, the modulation of these pathways will not only contribute to maintaining homeostatic regulation of the immune system but may also contribute to reducing cell apoptosis and necrosis. Other pathways involving T-helper cells, cytokine and chemokine signallers are also closely associated to enhance the immune system which could contribute to up-regulating the down-regulated immune system during corona infection [18-20].

Further, screening of multiple phytoconstituents from folk medicines using the network pharmacology approach identified β -maaliene to interact with the highest number of proteins from the JAK-STAT pathway. Based on the literature search, we did not found any reported anti-viral activity of β -maaliene; however, our prediction of biological spectrum via PASS ONLINE [21] predicted it to possess as an antiviral agent against influenza, adenovirus, CMV, Herpes, Picornavirus, and Hepatitis C. Further, the compound was also predicted as viral entry inhibitor. So, apart from modulating the proteins of the JAK-

STAT pathway, this agent may also act over the spike protein of coronavirus and inhibit it to enter into the cell. Further, these calculations suggest that analogs of β -maaliene could be the choice of investigative molecules as a modulator of the JAK-STAT pathway and inhibitor for virus entry into host cells.

During network pharmacology-evident target identification, we identified TRAF5 to be majorly modulated by the highest number of phytoconstituents. Previous reports suggest the requirement of TRAF5 to optimize the T cell expansion in response to infection [22]. Hence, we attempted to identify the lead hit agent as the prime modulator of this protein from the list of phytoconstituents. Based on the binding energy and number of hydrogen bond interactions we identified sesaminol 2-O- β -D-gentiobioside and vicenin-3 to possess the best interaction with TRAF5.

During this process, we also attempted to identify if the lead hits can interact with three major targets of coronavirus. Hence, ligand molecules that are interacting with the TRAF5 were docked with COVID-19 3clpro, PLpro and spike protein which identified sesaminol 2-O- β -D-gentiobioside, taxine B, vicenin-3, and sesaminol 2-O- β -D-glucoside as lead hits. Additionally, PASS ONLINE also predicted probable score for anti-viral activity of these lead hits against Influenza (Pa: 0.733), Hepatitis B (Pa: 0.402), and Herpes (Pa: 0.371) by sesaminol 2-O- β -D-gentiobioside(1), Rhinovirus (Pa:0.324) by Taxine B(2), Herpesvirus (Pa: 0.842), Influenza (Pa: 0.540), Hepatitis B virus (Pa: 0.443), Picornavirus (Pa: 0.349), Poxvirus (Pa: 0.237), Hepatitis (Pa: 0.136), and Retrovirus (Pa: 0.133) by vicenin-3 (3) and Influenza (Pa: 0.690), Hepatitis B (Pa: 0.378), Herpes (Pa: 0.396), Rhinovirus (Pa:0.305) by sesaminol 2-O- β -D-glucoside(4). Docking study showed the binding affinity of these molecules with 3clpro, PLpro and spike protein and these targets shared the domain with proteins involved with other viruses too; hence, these molecules can be further screened via their functional group modeling to target coronavirus.

Although, the present method of screening of anti-viral components plays an important role to identify lead hit anti-viral molecules; for the first time Indian herbal medications have been screened via this process i.e. network pharmacology and gene enrichment analysis. Further, the outcome of the present study is knowledge-based and is dependent upon multiple regression models for particular biological activities. On the other hand, during COVID-19 infection the dysregulated immune system may play important role in the spreading of the virus in the host system; could be maintained via the JAK-STAT signaling pathway which was the main basic concept of the present study. Likewise, identification of the homologous proteins may also play an important role in the identification of new drug molecules that kindled us for phylogeny comparison of targets which was based on the predeposited amino acid sequences of individual proteins.

5. Conclusion

The present study identified few lead hits from the traditional Indian medicines which were reported for their anti-viral property against a few well-known targets for coronavirus. However, the finding of the present study is a knowledge-based available database and computer simulations. Further investigations need to be made to confirm the findings accordingly.

Declarations

Conflict of interest

All the authors of this manuscript have no conflict of interest.

Funding

This work has not received any funds from national or international agencies.

Ethical statement

This article does not contain any studies with human participants or animals performed by any of the authors.

Data Availability

The raw data/results for the present study are freely available from Pukar Khanal (pukarkhanal58@gmail.com) upon request.

Author contribution

Pukar Khanal performed a review of the literature, mined the data, constructed the in-house database, performed the study, and drafted the manuscript. Taaza Duyu had an equal contribution in performing the study, drafting and reviewing the manuscript. BM Patil and Yadu Nandan Dey contributed to performing the review of literature, drafting and reviewing the manuscript. Ismail Pasha and Rohini S. Kavalapure contributed to the final refining of the manuscript.

References

1. H. Zhang, K. L. Wu, X. Zhang, S. Q. Deng, and B. Peng, "In silico screening of Chinese herbal medicines with the potential to directly inhibit 2019 novel coronavirus," *Journal of Integrative Medicine*, vol. 18, no. 2, pp.152-158, 2020.
2. WHO 2020, "Report of the WHO-China Joint Mission on Coronavirus Disease 2019 (COVID-19)," Available at: <https://www.who.int/docs/default-source/coronaviruse/who-china-joint-mission-on-covid-19-final-report.pdf> Accessed on: 27 March 2020
3. Li, Y. Fan, Y. Lai, T. Han, Z. Li, P. Zhou, P. Pan, W. Wang, D. Hu, X. Liu, and Q. Zhang, "Coronavirus infections and immune responses," *Journal of medical virology*, vol. 92, no.4, pp.424-432, 2020.
4. G. Bhoj, and Z. J. Chen, "Ubiquitylation in innate and adaptive immunity" *Nature*, vol. 458, no. 7237, pp.430–437, 2009.
5. A. Lindner, N. Fotouhi-Ardakani, V. Lytvyn, P. Lachance, T. Sulea, and R. Ménard, "The papain-like protease from the severe acute respiratory syndrome coronavirus is a deubiquitinating enzyme," *Journal of virology*, vol. 79, no.24, pp.15199-15208, 2005.

6. Li, M. J. Moore, N. Vasilieva, J. Sui, S. K. Wong, M. A. Berne, M. Somasundaran, J. L. Sullivan, K. Luzuriaga, T. C. Greenough, H. Choe, M. Farzan "Angiotensin-converting enzyme 2 is a functional receptor for the SARS coronavirus," *Nature*, vol.426, no. 6965, pp.450–454, 2003.
7. Lagunin, S. Ivanov, A. Rudik, D. Filimonov, and V. Poroikov, "DIGEP-Pred: web service for in silico prediction of drug-induced gene expression profiles based on structural formula," *Bioinformatics*, vol. 29, no.16, pp.2062-2063, 2013.
8. Szklarczyk, A. L. Gable, D. Lyon, A. Junge, S. Wyder, J. Huerta-Cepas, M. Simonovic, N. T. Doncheva, J. H. Morris, P. Bork, and L. J. Jensen, "STRING v11: protein–protein association networks with increased coverage, supporting functional discovery in genome-wide experimental datasets," *Nucleic acids research*, vol.47, no. D1, pp.D607-D613, 2019.
9. Shannon, A. Markiel, O. Ozier, N. S. Baliga, J. T. Wang, D. Ramage, N. Amin, B. Schwikowski, and T. Ideker, "Cytoscape: a software environment for integrated models of biomolecular interaction networks," *Genome research*, vol. 13, no. 11, pp. 2498-2504, 2003.
10. Yang, C. Lou, L. Sun, J. Li, Y. Cai, Z. Wang, W. Li, G. Liu, and Y. Tang, "admetSAR 2.0: web-service for prediction and optimization of chemical ADMET properties," *Bioinformatics*, vol. 35, no.6, pp.1067-1069, 2019.
11. Schwede, J. Kopp, N. Guex, and M.C. Peitsch, "SWISS-MODEL: an automated protein homology-modeling server," *Nucleic acids research*, vol. 31, no. 13, pp.3381-3385, 2003.
12. Discovery studio, 2019. Dassault Systèmes, San Diego, *Dassault Systèmes BIOVIA*, 2019.
13. A. Halgren, "Merck molecular force field. I. Basis, form, scope, parameterization, and performance of MMFF94," *Journal of Computational Chemistry*, vol. 17, pp.490–519, 1996.
14. M. Morris, R. Huey, W. Lindstrom, M. F. Sanner, R. K. Belew, D. S. Goodsell, and A. J. Olson, "AutoDock4 and AutoDockTools4: Automated docking with selective receptor flexibility," *Journal of Computational Chemistry*, vol. 30, no. 16, pp.2785-2791, 2009.
15. F. Altschul, T. L. Madden, A. A. Schäffer, J. Zhang, Z. Zhang, W. Miller, and D. J. Lipman, "Gapped BLAST and PSI-BLAST: a new generation of protein database search programs," *Nucleic Acids Research*, vol. 25, no. 17, pp. 3389-402, 1997.
16. S. Fung, and D. X. Liu, "Coronavirus infection, ER stress, apoptosis and innate immunity," *Frontiers in Microbiology*, vol. 5, Article ID 296, 2014.
17. Yue, N. R. Nabar, C. S. Shi, O. Kamenyeva, X. Xiao, I. Y. Hwang, M. Wang, and J.H. Kehrl, "SARS-Coronavirus Open Reading Frame-3a drives multimodal necrotic cell death," *Cell death & disease*, vol. 9 no. 9, pp.1-15, 2018.
18. Padovan, "Modulation of CD4+ T helper cell memory responses in the human skin," *International archives of allergy and immunology*, vol. 173, no. 3, pp.121-137, 2017.
19. Simon, "Immunomodulatory cytokines: directing and controlling immune activation," *Arthritis research & therapy*, vol. 13, no. 2, pp.014, 2011.
20. H. Jang, J. Y. Seoh, and M. Miyasaka, "Cytokines, chemokines, and their receptors: targets for immunomodulation," Conference report: International Cytokine Society Conference 2005. *Journal of*

leukocyte biology, vol.80, no. 2, pp.217-219, 2005.

21. Lagunin, A. Stepanchikova, D. Filimonov, and V. Poroikov, "PASS: prediction of activity spectra for biologically active substances," *Bioinformatics*, vol. 16, no. 8, pp.747-748, 2000.
22. J. Kraus, J. S. Haring, and G. A. Bishop, "TNF receptor-associated factor 5 is required for optimal T cell expansion and survival in response to infection," *The Journal of Immunology*, vol. 181, no. 11, pp.7800-7809, 2008.

Tables

Table 1: Enrichment analysis of modulated proteins from JAK-STAT pathway

Pathway ID	Pathway description	Observed gene count	Matching proteins in network	False discovery rate
hsa04917	Prolactin signaling pathway	5	CISH, KRAS, SOCS2, STAT5A, STAT5B	1.76E-07
hsa04630	Jak-STAT signaling pathway	5	CISH, MCL1, SOCS2, STAT5A, STAT5B	5.05E-06
hsa05221	Acute myeloid leukemia	4	BCL2A1, KRAS, STAT5A, STAT5B	5.95E-06
hsa05203	Viral carcinogenesis	4	KRAS, STAT5A, STAT5B, TRAF5	0.00023
hsa05223	Non-small cell lung cancer	3	KRAS, STAT5A, STAT5B	0.00033
hsa05220	Chronic myeloid leukemia	3	KRAS, STAT5A, STAT5B	0.00042
hsa04012	ErbB signaling pathway	3	KRAS, STAT5A, STAT5B	0.00046
hsa04933	AGE-RAGE signaling pathway in diabetic complications	3	KRAS, STAT5A, STAT5B	0.00065
hsa04210	Apoptosis	3	BCL2A1, KRAS, MCL1	0.0015
hsa05161	Hepatitis B	3	KRAS, STAT5A, STAT5B	0.0015
hsa04217	Necroptosis	3	STAT5A, STAT5B, TRAF5	0.0018
hsa05200	Pathways in cancer	4	KRAS, STAT5A, STAT5B, TRAF5	0.004
hsa05166	HTLV-I infection	3	KRAS, STAT5A, STAT5B	0.006
hsa04658	Th1 and Th2 cell differentiation	2	STAT5A, STAT5B	0.0136
hsa04064	NF-kappa B signaling pathway	2	BCL2A1, TRAF5	0.0141
hsa04659	Th17 cell differentiation	2	STAT5A, STAT5B	0.0158
hsa04140	Autophagy - animal	2	DEPTOR, KRAS	0.022
hsa04910	Insulin signaling pathway	2	KRAS, SOCS2	0.0234
hsa05162	Measles	2	STAT5A, STAT5B	0.0234
hsa04150	mTOR signaling pathway	2	DEPTOR, KRAS	0.0258
hsa05206	MicroRNAs in cancer	2	KRAS, MCL1	0.0258
hsa04360	Axon guidance	2	KRAS, RASA1	0.0316

hsa04062	Chemokine signaling pathway	2	KRAS, STAT5B	0.0329
hsa04014	Ras signaling pathway	2	KRAS, RASA1	0.0489

Table 2: Druglikeness of phytoconstituents targeting TRAF5

Compound	Molecular formula	Molecular weight	NHBA	NHBD	MolLogP	MolLogS (Log(moles/L))	DLS
α -gurjunene	C ₁₅ H ₂₄	204.19	0	0	5.03	-4.81	-1.18
-garcinia acid	C ₆ H ₆ O ₇	190.01	7	3	-2.25	-0.18	-0.92
-3,7-dihydroxychroman-4-ol	C ₉ H ₈ O ₄	180.04	4	2	0.28	-2.07	0.24
-acetyl-4R,6S-epi-sativanolactone	C ₁₇ H ₂₄ O ₅	308.16	5	1	1.88	-1.51	0.08
leoxyepisappanol	C ₁₆ H ₁₆ O ₅	288.10	5	4	1.50	-1.38	-0.09
leoxysappanol	C ₁₆ H ₁₆ O ₅	288.10	5	4	1.50	-1.38	-0.09
laaliene	C ₁₅ H ₂₄	204.19	0	0	4.95	-4.70	-0.51
zilein	C ₁₆ H ₁₂ O ₅	284.07	5	3	1.01	-2.37	-0.56
zilin	C ₁₆ H ₁₄ O ₅	286.08	5	4	1.68	-1.58	-0.49
esalpinin C	C ₂₄ H ₃₂ O ₆	416.22	6	1	3.46	-3.32	-0.16
esalpinin D	C ₂₄ H ₃₀ O ₈	446.19	8	1	2.34	-2.40	-0.48
esalpinin F	C ₂₃ H ₃₀ O ₇	418.20	7	1	2.59	-2.73	0.33
uradiol	C ₃₀ H ₅₀ O ₂	442.38	2	2	6.78	-5.91	-0.04
ta-elemene	C ₁₅ H ₂₄	204.19	0	0	5.51	-5.41	-1.19
eanothic acid	C ₃₀ H ₄₆ O ₅	486.33	5	3	5.36	-5.13	0.19
antinine F	C ₂₂ H ₂₆ N ₂ O ₅	398.18	6	2	2.33	-2.80	0.31
ngiferin	C ₁₉ H ₁₈ O ₁₁	422.08	11	8	-0.13	-1.49	0.25
caesalpinin A	C ₂₃ H ₃₀ O ₇	418.20	7	1	2.38	-2.52	0.26
caesalpinin B	C ₂₃ H ₃₀ O ₇	418.20	7	1	2.55	-2.53	0.20
caesalpinin D	C ₂₅ H ₃₂ O ₉	476.20	9	1	2.15	-2.37	0.17
caesalpinin E	C ₂₁ H ₂₈ O ₆	376.19	6	2	1.89	-2.23	0.55
tanic acid	C ₂₉ H ₄₆ O ₄	458.34	4	2	4.82	-4.38	0.58
indifuran	C ₂₂ H ₃₄ O ₄	362.25	4	1	4.67	-4.45	0.17
cifoliol	C ₁₃ H ₁₄ O ₅	250.08	5	1	0.62	-1.45	0.06

daracopimaric acid	C ₂₀ H ₃₀ O ₂	302.22	2	1	4.48	-4.40	-0.55
acic acid	C ₁₀ H ₁₈ O ₄	202.12	4	2	1.37	-1.31	-0.01
aminol	C ₂₀ H ₁₈ O ₇	370.11	7	1	3.02	-2.71	-0.55
aminol 2-O-β-D- tiobioside	C ₃₂ H ₃₈ O ₁₇	694.21	17	7	-0.88	-1.19	-0.23
aminol 2-O-β-D- coside	C ₂₆ H ₂₈ O ₁₂	532.16	12	4	0.99	-1.30	-0.26
mastane-3β,5α,6β- l	C ₂₉ H ₅₂ O ₃	448.39	3	3	6.52	-6.05	0.56
ine B	C ₃₃ H ₄₅ NO ₈	583.31	9	3	2.24	-2.61	0.82
enin-3	C ₂₆ H ₂₈ O ₁₄	564.15	14	10	-0.52	-1.43	0.32
agnusin I	C ₂₂ H ₃₄ O ₆	394.24	6	2	3.26	-3.55	0.71
trifolin D	C ₂₄ H ₃₈ O ₅	406.27	5	1	4.83	-4.43	0.82
ex norditerpenoid 1	C ₁₉ H ₃₀ O ₂	290.22	2	0	3.93	-3.98	-0.57
ex norditerpenoid 2	C ₂₁ H ₃₂ O ₄	348.23	4	0	3.85	-3.75	0.30
exilactone	C ₂₂ H ₃₄ O ₅	378.24	5	1	3.55	-3.86	0.88
berellin A45	C ₁₉ H ₂₄ O ₅	332.16	5	2	1.23	-1.40	-0.60
berellin A63	C ₁₉ H ₂₄ O ₆	348.16	6	3	0.34	-0.78	-0.59

NHBA: Number of hydrogen bond acceptors, NHBD: Number of hydrogen bond donors, DLS: Druglikeness Score

Table 3: Binding energy and mode of interactions of phytoconstituents with TRAF5

Ligand	Binding Affinity (Kcal/mol)	NHB	HBR
(S)-3,7-dihydroxychroman-4-one	-5.1	-	-
1-O-acetyl-4R,6S-britannilactone	-5	3	GLN431, SER430, PHE429
3'-deoxyepisappanol	-6.5	3	TYR402, TYR434, ARG393
3'-deoxysappanol	-5.9	2	GLN431, GLY399
Norcaesalpinin A	-6.6	3	LYS416, GLN431
Norcaesalpinin B	-6.3	3	SER505, GLY520, CYS521
Vitex norditerpenoid 1	-6.2	1	ARG441
Vitex norditerpenoid 2	-6.5	1	CYS443
Brazilein	-6.5	1	ASN535
Brazilin	-6.6	1	GLU531
Caesalpinin C	-6.2	2	ARG418, LYS414
Caesalpinin D	-7.7	4	GLN431, THR411
Caesalpinin F	-6.1	4	SER505, SER507, SER519
Daturadiol	-8.4	-	-
δ -Elemene	-5.3	-	-
Isoceanothic Acid	-7.2	2	ARG441, GLN431
Jerantinine F	-6.6	1	LYS416
Mangiferin	-7.3	3	TRP408, GLN431, GLY399
Norcaesalpinin D	-5.4	1	LYS509
Norcaesalpinin E	-6.1	1	ASP541
Platanic acid	-7.5	2	THR411, LYS416
Rotundifuran	-5.7	2	TRP408, LYS395
Salicifoliol	-5.8	2	TRP408, GLY399
Sandaracopimaric Acid	-7.2	1	ASP540
Sebacic Acid	-4.1	2	GLU531, LYS414
Sesaminol	-7.6	-	-

Taxine B	-6.4	3	GLN431, THR411, TRP408
Vicenin-3	-6.6	9	LYS500, ASP502, SER505, SER506, SER507, GLY520, SER519
Viteagnusin I	-6.7	1	LYS417
Vitetrifolin D	-5.6	-	-
Vitexilactone	-6.5	1	GLU531
(+)-garcinia acid	-5.1	5	VAL421, ASN449, GLY450
(-)- α -gurjunene	-5.5	-	-
β -maaliene	-6.6	-	-
Gibberellin A45	-6.9	1	SER432
Gibberellin A63	-7.5	3	THR411, LYS409
Sesaminol 2-O- β -D-gentiobioside	-8.6	5	GLN431, PHE429, TRP408
Sesaminol 2-O- β -D-glucoside	-7.8	8	LYS416, LYS409, TRP408, PHE429, LYS395
Stigmastane-3 β , 5 α , 6 β -triol	-6.4	2	GLN431

NHB: Number of hydrogen bonds, HBR: Hydrogen bond residues

Table 4: Binding energy and mode of interaction of phytoconstituents with 3clpro

and	Binding energy (kcal/mol)	NHB	HBR
-garcinia acid	-5.6	5	GLN110, ASN151, THR111
α -gurjunene	-6.4	-	-
-3 7-dihydroxychroman-4-	-5.8	4	GLN110, THR111, ASP153, SER158
-acetyl-4R, 6S- annilactone	-5.8	5	ASN277, GLY278, ALA285, TYR239, THR199
leoxyepisappanol	-6.5	2	ASN142, GLU166
leoxysappanol	-6.7	-	-
caesalpinin A	-7.1	4	THR111, GLN110
caesalpinin B	-7.4	2	THR292, GLN110
ox norditerpenoid 1	-6.8	3	GLN110, THR292, THR111
ox norditerpenoid 2	-7	5	LYS102, SER158, THR111, THR292, GLN110
aaaliene	-6	-	-
zilein	-7.3	4	GLN110, THR111, ASP295
zilin	-7.1	2	SER158, THR111
esalpinin C	-6.7	3	TYR239, THR199
esalpinin D	-7.1	3	LEU287, TYR239, TYR237
esalpinin F	-6.7	1	GLU166
uradiol	-8	2	ASP197, ASN238
lemene	-5.4	-	-
berellin A45	-7.6	3	GLN110, THR111, ASN151
berellin A63	-7.4	5	ASN238, THR199, ASP289
eanothic acid	-7.7	2	GLU166, HIS164
antinine F	-7.5	-	-
ngiferin	-8.5	5	THR190, SER144, HIS41, ASN142
caesalpinin D	-6.7	3	LEU287, ARG131, THR199
caesalpinin E	-6.9	5	GLY195, ASP197, ASN238, LYS137, THR135

anic acid	-8.3	2	LEU271, THR199
undifuran	-6.6	2	ASN151, GLN110
icifoliol	-6.5	3	GLY143, SER144, CYS145
idaracopimaric acid	-6.5	-	-
iacic acid	-4.7	2	ASN151, THR111
aminol 2-O-β-D- tiobioside	-8.7	2	GLU166, THR190
aminol 2-O-β-D-glucoside	-9.2	2	GLU166, THR190
aminol	-7.9	4	LYS137, ARG131, TYR239
ymastane-3β,5α,6β-triol	-6.5	3	LEU287, TYR239
ine B	-7.9	3	PHE294, GLN110
enin-3	-8.2	5	GLY143, SER144, GLU166
agnusin I	-6.7	4	THR199, LYS137, ARG131, GLU288
trifolin D	-6.2	4	ARG131, THR199
xilactone	-6.9	1	GLN110

NHB: Number of Hydrogen Bonds, HBR: Hydrogen Bond Residues

Table 5: Binding energy and mode of interaction of phytoconstituents with PLpro

gand	Binding (kcal/mol)	Affinity	NHB	HBR
-)-garcinia acid	-5.5		4	GLY272, TYR265, GLY164
)- α -gurjunene	-6		-	-
)-3, 7-dihydroxychroman-4- ne	-5.7		-	-
O-acetyl-4R, 6S- itannilactone	-7		2	TYR269, GLY272
-deoxyepisappanol	-6.6		1	TYR269
-deoxysappanol	-6.8		1	GLY164
orcaesalpinin A	-6.7		5	ASN178, SER181, ALA182
orcaesalpinin B	-7.3		5	TYR252, SER213, ASP215, TYR214
tex norditerpenoid 1	-6.2		1	TYR306
tex norditerpenoid 2	-6		-	-
maaliene	-5.8		-	-
razilein	-8		-	-
razilin	-7.5		4	THR55, TYR36, GLY39, ARG139
aesalpinin C	-7.1		2	TYR265, TYR269
aesalpinin D	-7.9		2	TYR274, TYR265
aesalpinin F	-6.4		-	-
aturadiol	-7.8		2	GLN233, MET207
elemene	-5.3		-	-
bberellin A45	-6.9		3	TYR265, ASP165
bberellin A63	-7.3		-	-
oceanothic Acid	-7		4	SER310, GLU308, THR309, ASP215
rantine F	-6.6		1	PHE259
angiferin	-7.3		1	SER181
orcaesalpinin D	-6.1		3	ARG167, GLN233, TYR208
orcaesalpinin E	-7.3		3	TYR265, TYR274
atonic acid	-7.1		2	GLN233
otundifuran	-6.9		4	LYS158, TYR269, TYR265, THR302

alicifoliol	-7.1	2	THR302, TYR274
andaracopimaric Acid	-6.7	1	TYR269
ebacic acid	-5.4	1	THR302
esaminol 2-O-β-D- entiobioside	-8.5	4	THR75, ASP77
esaminol 2-O-β-D-glucoside	-7.5	4	LYS218, PHE259, LYS280, ALA279
esaminol	-8.2	2	TYR265, TYR269
igmastane-3β,5α,6β-triol	-6.2	4	GLN233, TYR208, MET209
ixine B	-6.9	6	THR171, ARG167, GLU204, MET207, GLN233
enin-3	-6.9	2	SER181, SER241
teagnusin I	-7.4	4	TYR265, LYS158, TYR274, THR302
tetrifolin D	-6.4	2	ARG167, TYR265
texilactone	-7.3	3	LYS158, THR302, TYR265

NHB: Number of hydrogen bonds, HBR: Hydrogen bond residues

Table 6: Binding energy and mode of interaction of phytoconstituents with spike protein

and	Binding Affinity (kcal/mol)	NHB	HBR
-garcinia acid	-5.7	5	TYR66, THR94, ASN185, ALA255
α -gurjunene	-6.6	-	-
-3,7-dihydroxychromanone	-6.2	2	ALA608, TYR588
-acetyl-4R,6S-annilactone	-6	2	THR525, ARG314
leoxyepisappanol	-7.1	1	ASP595
leoxysappanol	-7	2	ILE600, ILE611
caesalpinin A	-6.7	3	ARG77, ASP137, TYR136
caesalpinin B	-7	1	ALA259
ex norditerpenoid 1	-6.5	-	-
ex norditerpenoid 2	-6.7	3	THR94, TYR66, ALA255
aaaliene	-6.3	-	-
zilein	-7	2	ILE881, HIS1020
zilin	-6.8	4	GLY716, ASP717, LEU938, ARG972
esalpinin C	-6.7	2	TYR136
esalpinin D	-7.4	4	LEU493, ASN495, SER490, ARG350
esalpinin F	-6.6	4	TYR136, ASP137, TYR139
uradiol	-8.2	1	ASP820
lemene	-5.3	-	-
berellin A45	-6.9	1	LYS807
berellin A63	-7.2	-	-
eanothic acid	-7.7	4	THR799, GLN304, SER300, SER302
antinine F	-7.1	2	ALA287, LEU288
ngiferin	-8	3	ALA801, PHE805, ASP46
caesalpinin D	-7.3	1	GLN825
caesalpinin E	-6.8	2	GLN825, ASP811
tanic acid	-7.9	1	ARG268

undifuran		-6.2	2	ILE600, LYS266
icifoliol		-6.1	-	-
daracopimaric acid		-8.3	-	-
oacic acid		-4.1	3	ARG77, TYR139, ALA156
aminol tiobioside	2-O-β-D-	-9.7	8	THR47, LEU48, GLN825, ALA801, ALA803, PHE805, LYS807, ASP811
aminol coside	2-O-β-D-	-7.9	3	LYS705, THR831, ILE816
aminol		-7.7	3	SER460, TRP348, ASN417
ymastane-3β,5α,6β-triol		-7.8	1	TYR59
ine B		-8.1	1	THR47
enin-3		-8	4	TYR59, ILE600, ALA287, THR599
agnusin I		-7.4	2	THR47, LEU48
ertrifolin D		-6.2	5	ASP46, ASP811, GLN825
exilactone		-6.9	4	LEU48, THR47, GLY814, LYS807

NHB: Number of hydrogen bonds, HBR: Hydrogen bond residues

Figures

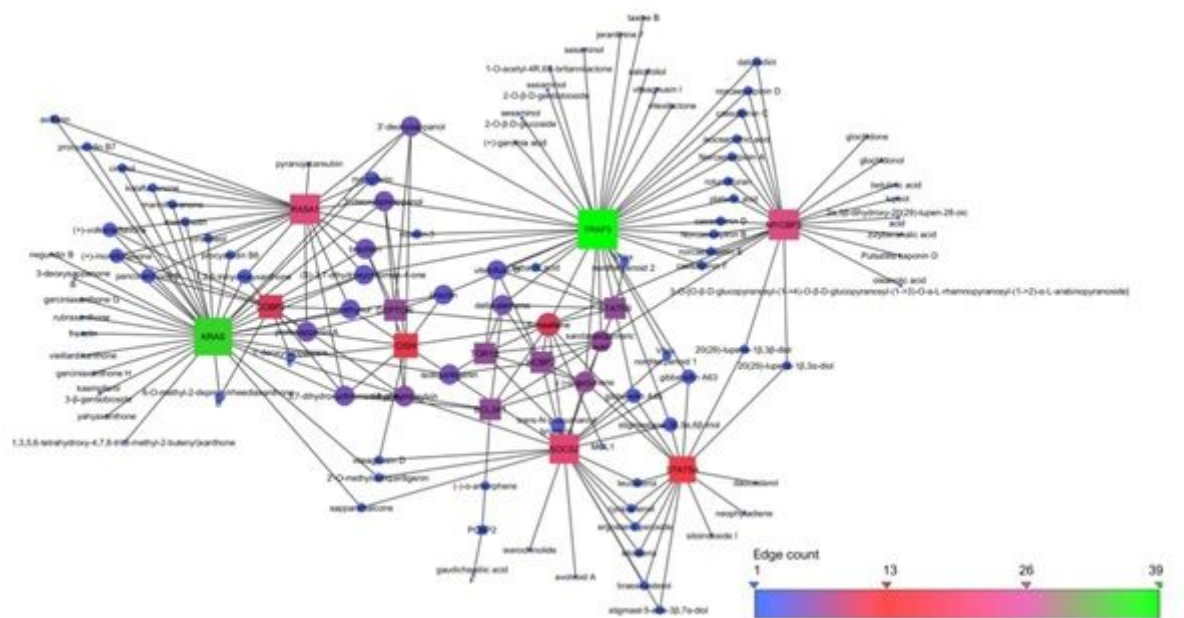


Figure 1

Interaction of phytoconstituents with proteins involved in JAK-STAT pathway

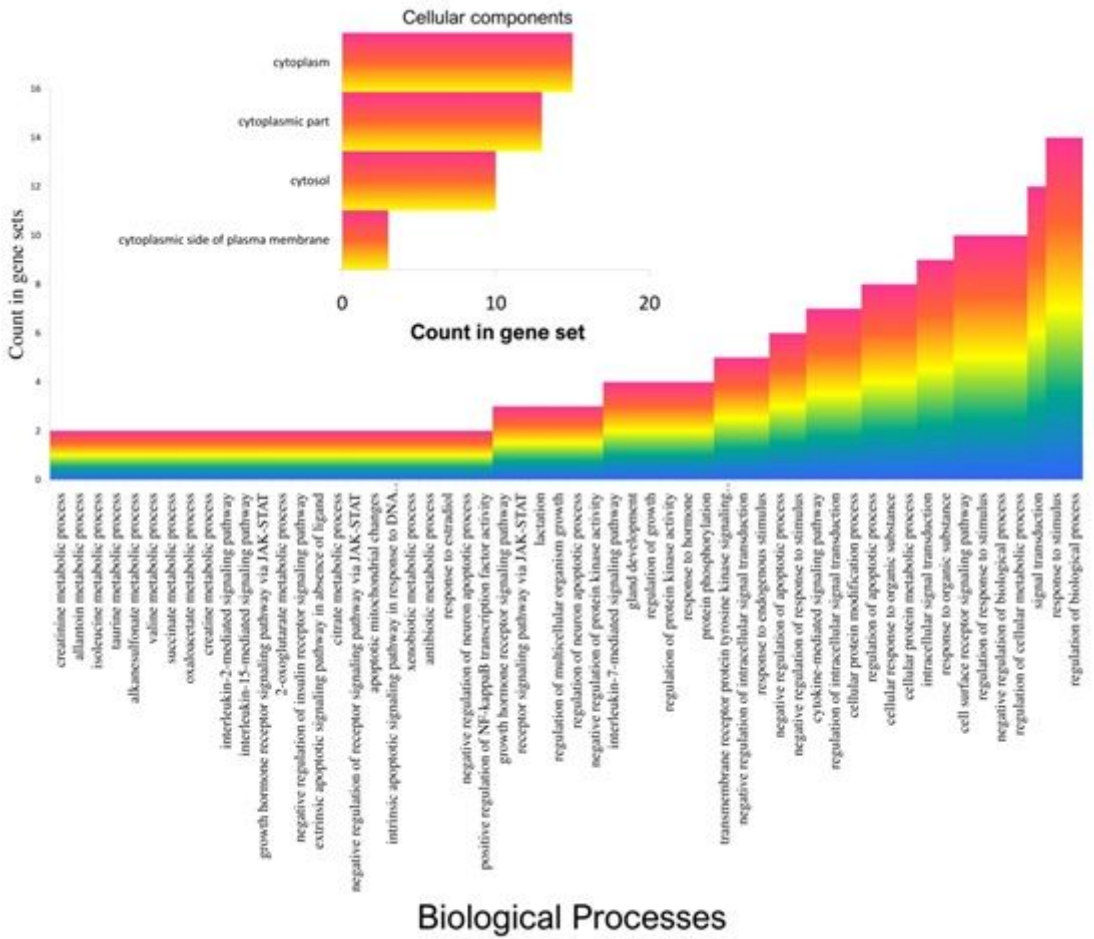


Figure 2

Gene GO analysis of proteins from JAK-STAT pathway

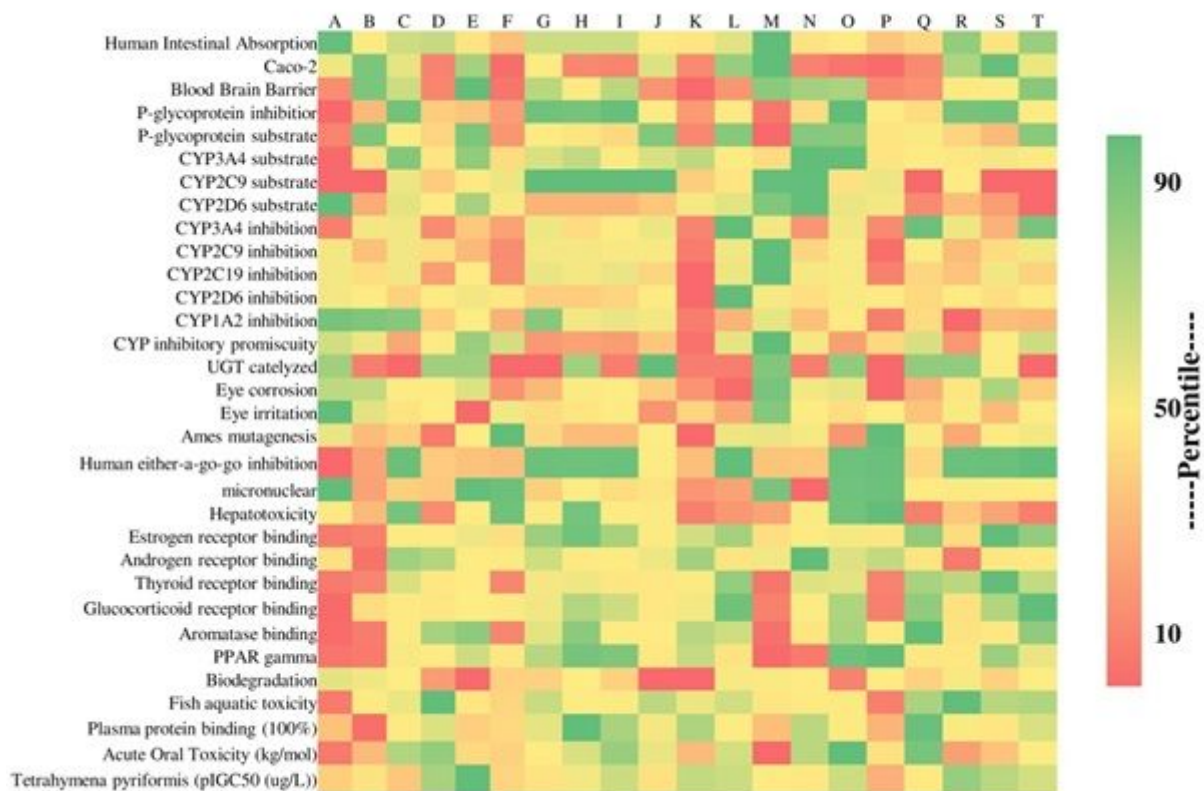


Figure 3

ADMET Profile of phytoconstituents (A) (S)-3,7-dihydroxychroman-4-one, (B) 1-O-acetyl-4R,6S-britannilactone, (C) caesalpinin F, (D) isoceanothic acid, (E) jerantinine F, (F) mangiferin, (G) Norcaesalpinin A, (H) Norcaesalpinin B, (I) norcaesalpinin D, (J) norcaesalpinin E, (K) platanic acid, (L) rotundifuran, (M) salicifoliol, (N) stigmastane-3 β ,5 α ,6 β -triol, (O)taxine B, (P) vicenin-3, (Q) viteagnusin I, (R) vitetrifolin D, (S) Vitex norditerpenoid 2, and (T) vitexilactone

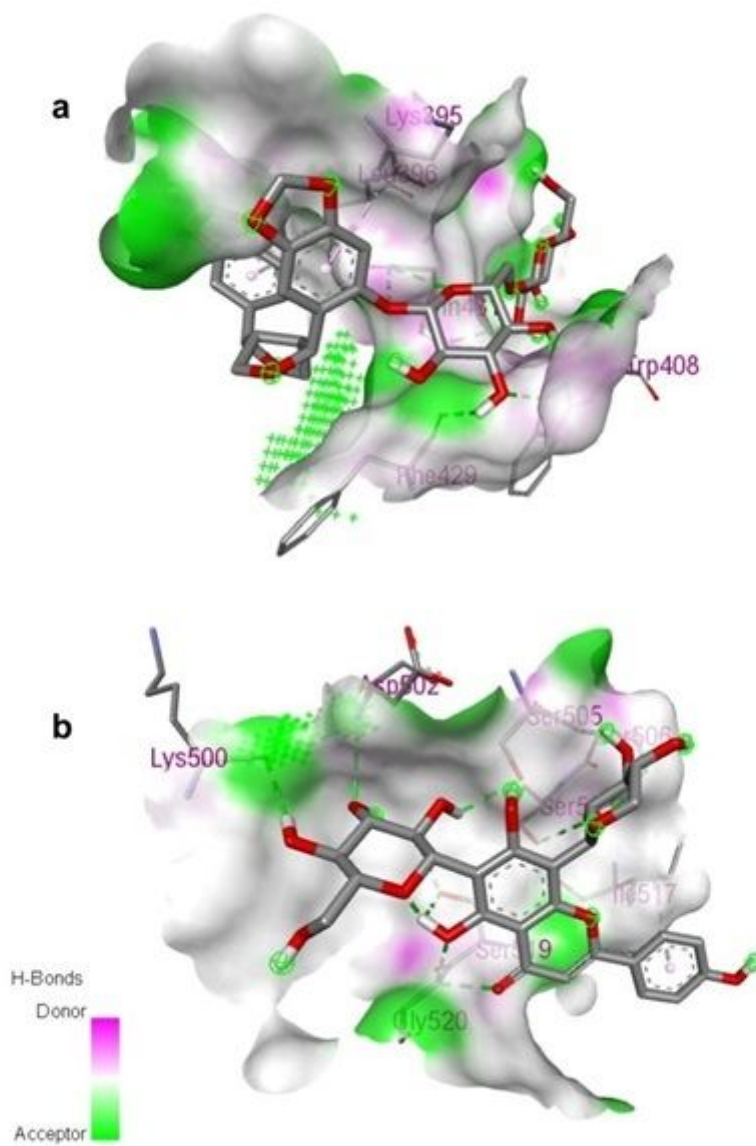


Figure 4

Interaction of (a) sesaminol_2-O- β -D-gentiobioside and (b) vicenin-3 with TRAF5

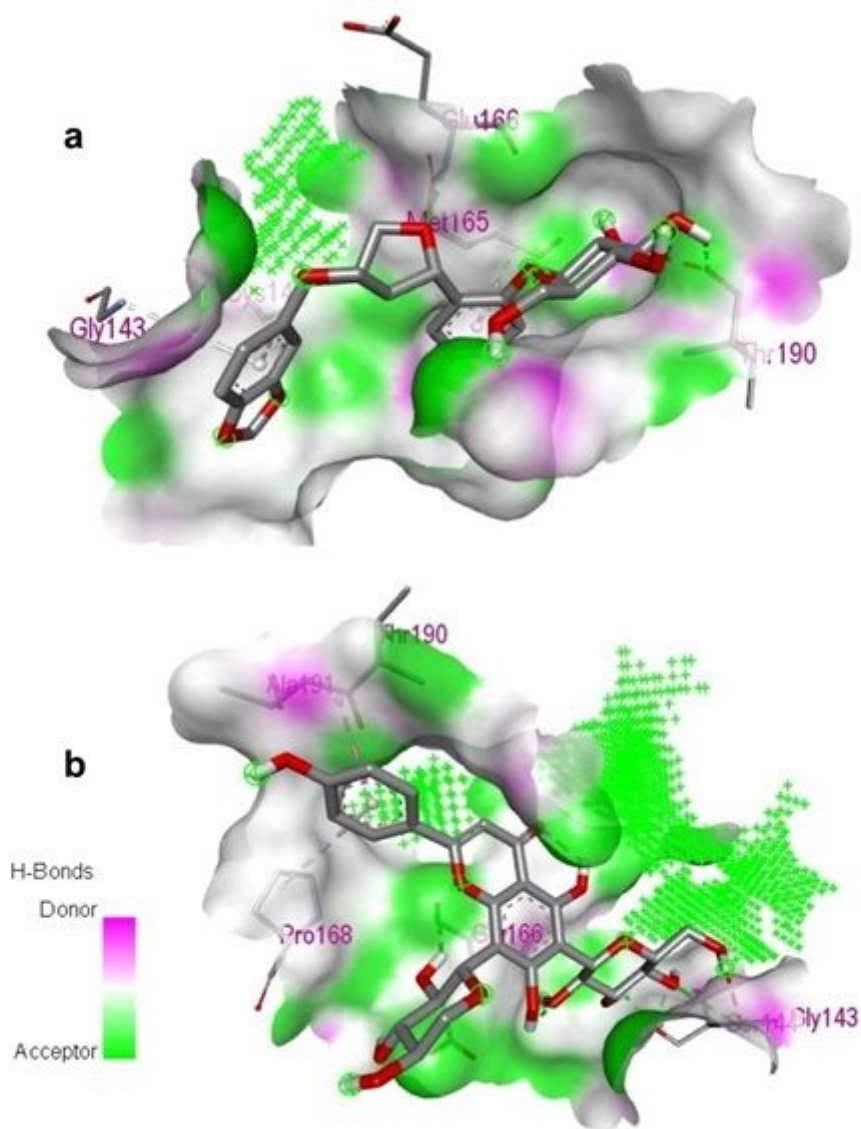


Figure 5

Interaction of (a) sesaminol_2-O- β -D-glucoside and (b) vicenin-3 with 3clpro

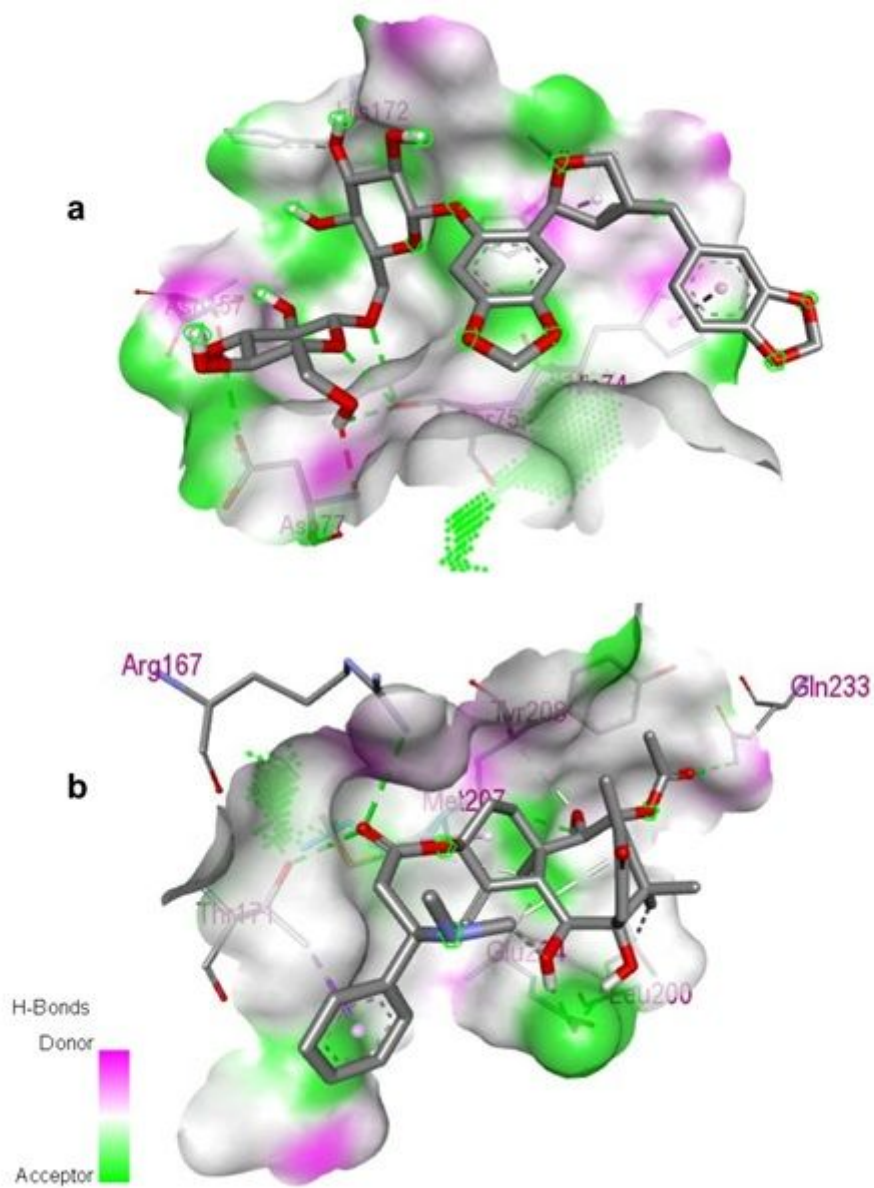


Figure 6

Interaction of (a) sesaminol_2-O-β-D-gentiobioside and (b) taxine B with PLpro

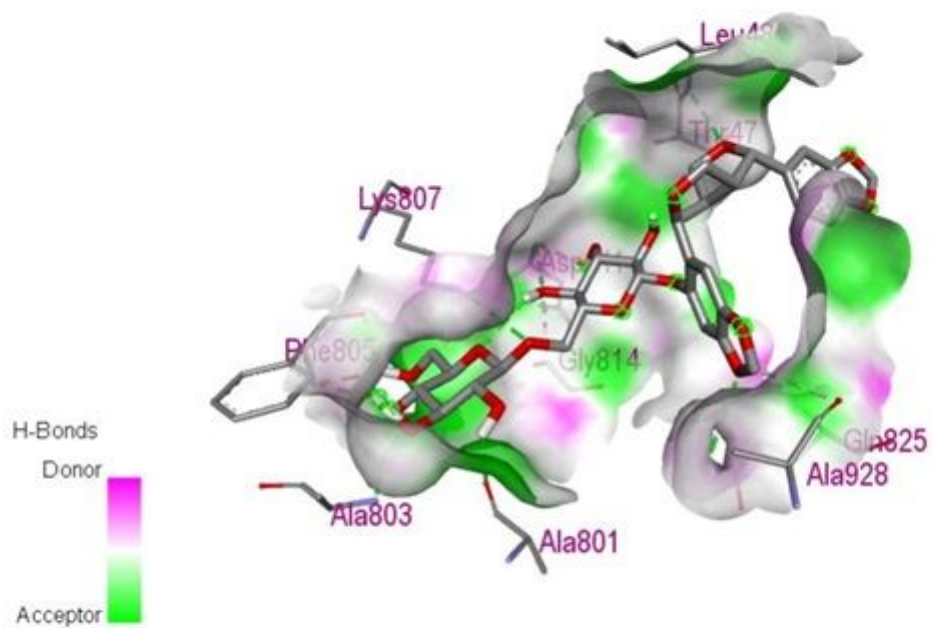


Figure 7

Interaction of sesaminol 2-O-β-D-gentiobioside with spike protein

